

**Solvent Effects on the Structural, Electronic, Non-Linear Optical  
and Thermodynamic Properties of Perylene Based on Density  
Functional Theory**

**Abstract:**

Perylene ( $C_{20}H_{12}$ ) is an important member of the polycyclic aromatic hydrocarbons (PAHs) that has a wide applications such as organic photovoltaic cells, field effect transistors and biosensors. Optimized bond lengths and bond angles, HOMO-LUMO energy gap, global chemical indices, total energy, nonlinear optical and thermodynamic properties of Perylene in the gas phase and in solvents (water, chloroform, benzene and acetone) were obtained based on Density Functional Theory with B3LYP/6-311++G(d,p) basis set. All the computations were carried out using Gaussian 03 package and revealed that the solvents have an effect on the optimized parameters. It was observed that the bond lengths increase with an increase in the polarity of the solvents, while the bond angles were found to increase as the polarity of the solvents decreases. Perylene molecule was found to have a higher stability in the gas phase with HOMO-LUMO energy gap of 2.9935eV. The HOMO and HOMO-LUMO energy gap were found to increase with an increase in polarity of the solvents. The molecule was found to be harder and less reactive in the gas phase with chemical hardness of 1.4968eV. The maximum value of ionization potential 5.3227eV and minimum value of electron affinity 2.2757eV were obtained in water and gas phase respectively, as such it is difficult to remove an electron from the molecule in water to form an ion and it is also difficult to add an electron to the molecule in gas phase. The ground state total energy of the molecule was found to increase with an increase in polarity of the solvents. Similarly, the chemical hardness, chemical softness, electronegativity, chemical potential and electrophilicity index were found to increase with an increase in the dielectric constant of the solvents. In the non-linear optical (NLO) properties calculations, it was observed that Perylene is a neutral molecule. It was found that the specific heat capacity of perylene increases with an increase in the polarity of the solvent while the entropy and the zero-point vibrational energy of the molecule decreases as the polarity of the solvent increases. In the non-linear optical properties calculations, it was found that the polarizability ( $\langle\alpha\rangle$ ) of Perylene increases with decrease in the polarity of the solvents and the anisotropic polarizability ( $\Delta\alpha$ ) of Perylene increase with an increase in the polarity of the solvents. In the Natural Bond Orbital (NBO) analysis, high intensive interaction between donor and acceptor electrons of Perylene was observed in chloroform due to large stabilization energy of 4.49Kcal/mol. The result shows that careful selection of the solvents and basis sets can tune the frontier molecular molecular orbital energy gap.

**KEYWORDS:** Density Functional Theory, Gaussian 03, HOMO-LUMO, Non-linear Optical Properties and Perylene.

## 40 1.INTRODUCTION

41 With rising demand for sustainably risk free energy, there is no better alternative than organic  
42 electronic materials which have proved to be a promising candidates for advanced optoelectronic  
43 applications such as in light emitting diodes, photovoltaic cells [1], organic field effect  
44 transistors, organic solar cells and transparent white displays [2, 3]. To fully understand and use  
45 these materials, their basic fundamental physical properties must be sufficiently explored. To  
46 acquire such vital information, their structural, electronic, optical, non-linear optical and  
47 thermodynamic properties are required.

48 Rylene are series of polycyclic aromatic hydrocarbons (PAHs) with general chemical formula  
49  $C_{10n}H_{4n+4}$  among which are the most widely investigated perylene ( $C_{20}H_{12}$ ) and its derivatives  
50 such as pyrenebisimides, perylene tetracarboxylic acid (PTDCA) and perylene-3,4,9,10-  
51 tetracarboxylic anhydride (PDA) which, due to their promising electronic, optical and charge-  
52 transport properties, are widely used in high-tech applications such as organic photovoltaic,  
53 organic field effect transistors, biolabels, sensors, single molecular spectroscopy, super  
54 molecular assemblies and opto-electronic devices [4].

55 Interestingly, wide ranges of experimental and theoretical studies have explored the synthesis  
56 and applications of perylene and its derivatives including Density Functional Theory. For  
57 instance, [5] presented within the framework of Density Functional Theory (DFT) as well as a  
58 comparative study of the electronic, optical, and transport properties of some selected polycyclic  
59 aromatic hydrocarbons (Perylene included). Similarly, the structural, and optoelectronic  
60 properties of different classes of perylene: isolated perylene, diindol[1,2,3-cd:1',2',3'-  
61 Im]perylene (DIP) molecule and DIP molecular crystal were investigated [6]. The effect of  
62 aggregation on the excited-state electronic structure of Perylene through transient absorption  
63 measurements of isolated molecules, excimers in solution, monomeric crystal forms ( $\beta$ -  
64 perylene), and dimeric crystal forms ( $\alpha$ -perylene) were studied [7]. The aggregation of water  
65 soluble, dicationic Perylene bisimide derivatives using absorption and emission spectroscopies,  
66 X-ray and neutron scattering techniques as well as electron microscopy, provides evidence for  
67 the existence of higher order molecular aggregates in solution [2]. The structure and electronic

68 properties of pyrene and coronene under pressure were also theoretically investigated using  
69 DFT [8] and Van der Waals interaction which were also used in obtaining the electronic structure  
70 of crystalline perylene [9]. However, to the best of our knowledge, the effects of solvents on this  
71 promising organic material have never been studied before. In the present investigation,  
72 computational studies have been carried out to investigate the effects of solvents on the  
73 structural, electronic, thermodynamic and non-linear optical properties of Perylene based on  
74 density functional theory.

75 Choice of a suitable solvent is of paramount scientific interest to obtain desired efficiency,  
76 selectivity and kinetics of chemical reaction [10]. The solvents used in this work include Water,  
77 Chloroform, Benzene and Acetone with the following dielectric constants; Water ( $\epsilon = 80.37$ ),  
78 Chloroform ( $\epsilon = 4.806$ ), Benzene ( $\epsilon = 2.284$ ) and Acetone ( $\epsilon = 37.50$ ).

## 79 2. THEORETICAL BACKGROUND

### 80 2.1 Density Functional Theory

81 Density Functional Theory is a phenomenally successful approach to finding solutions to the  
82 fundamental equation that describes the quantum behavior of atoms and molecules [11]. DFT has  
83 proved to be highly successful in describing structural and electronic properties in a vast class of  
84 materials, ranging from atoms and molecules to simple crystals to complex systems [12]. Density  
85 functional theory (DFT) was proposed by Hohenberg and Khon as a method to determine the  
86 electronic structure of a system at ground state with a theory stating that all ground state  
87 properties for many particle systems are functional of the electron density [13, 14]. In 1965,  
88 Khon and Sham (KS) reformulated the problem in a more familiar form and opened the way to  
89 practical application of DFT [12]. For a system of non-interacting electrons, the ground state  
90 charge density is representable as a sum over one-electron orbitals (KS orbitals)  $n(r)$  [12]. That  
91 is;

$$92 \quad n(r) = 2 \sum_i |\Psi_i(r)|^2 \quad (1)$$

93 If we assume double occupancy of all states, and the Khon-Sham orbitals are the solution to the  
94 Schrodinger equation.

95 
$$\left[-\frac{\hbar^2}{2m}\nabla^2 + V_{KS}(r)\right]\Psi_i(r) = \epsilon_i \Psi_i(r) \quad (2)$$

96 where,

97 
$$V_{KS} = V_{ext} + \int \frac{e^2 n(r)n(r')}{|r-r'|} drdr' + V_{XC}[n(r)] \quad (3)$$

98 is a unique potential having  $n(r)$  as its charge density. Thus we have;

99 
$$\left(-\frac{\hbar^2}{2m}\nabla^2 + V_H(r) + V_{XC}[n(r)] + V(r)\right)\Psi_i(r) = \epsilon_i \Psi_i(r) \quad (4)$$

100 where,  $V_H(r)$  is the Hartree potential and  $V_{XC}[n(r)]$  is the exchange correlation potential.

101 A wide variety of different approximations have been developed to take care of the effects of  
 102 electron-electron interactions such as the generalized gradient approximation (GGA), local  
 103 density approximation (LDA) and Hybrid Approximations.

104 In the LDA, the exchange correlation energy at a point in space is taken to be that of the  
 105 homogeneous electron gas with local-density  $\epsilon_{XC}(n)$ . Thus the total exchange correlation  
 106 energy functional is approximated as [15];

107 
$$E_{XC}^{LD} = \int n(r) \epsilon_{XC}(n(r)) dr \quad (5)$$

108 From which the potential is obtained as;

109 
$$V_{XC} = \frac{\delta E_{XC}}{\delta n} \quad (6)$$

110 where,  $\delta E_{XC}$  and  $\delta n$  are the derivatives of the exchange energy and the electron density  
 111 respectively.

112 Whereas, the generalized gradient approximation (GGA) depends on both local density and it's  
 113 gradient, it can be expressed as;

114 
$$E_{XC}^{GGA} = \int n(r) \epsilon_{XC}(n|\nabla n|\nabla^2 n) dr \quad (7)$$

115 where,  $n(r)$  is the electron density.

116 Unlike LDA and GGA, the hybrid function is a linear combination of Hartree-Fock exchanges  
117 expressed as [15]:

$$118 \quad E_{XC}^{hybrid} = \alpha E_{XC}^{HF} + E_C \quad (8)$$

119 where  $E_{XC}^{HF}$  is the Hartree-Fock exchange energy and  $\alpha$  can be chosen to satisfy particular criteria.

## 120 2.2 Global Quantities

121 Global reactivity descriptors such as chemical potential, chemical hardness-softness,  
122 electronegativity and electrophilicity index are useful quantities in predicting and understanding  
123 global chemical reactivity trends. The ionization potentials (IP) and electron affinities (EA) of  
124 the molecule in the gas phase and in solvents are computed using Koopman's Hypothesis,  
125 through the HOMO and LUMO energy orbitals respectively using the following expressions;

$$126 \quad IP = -E_{HOMO} \quad (9)$$

$$127 \quad EA = -E_{LUMO} \quad (10)$$

128 The difference between the highest occupied molecular orbital (HOMO) and lowest unoccupied  
129 molecular orbital (LUMO) known as energy gap can be obtained from the relation;

$$130 \quad E_{gap} = E_{LUMO} - E_{HOMO} \approx IP - EA \quad (11)$$

131 Chemical hardness is given by half of the energy band gap [16];

$$132 \quad \eta = \frac{IP - EA}{2} \quad (12)$$

133 The softness of a molecule can be obtained by taking the inverse of its chemical hardness [17];

$$134 \quad S = \frac{1}{\eta} \quad (13)$$

135 The chemical potential is given by [17];

$$136 \quad \mu = -\left(\frac{IP + EA}{2}\right) \quad (14)$$

137 The electronegativity is given by [17];

138 
$$\chi = \frac{IP+EA}{2} \quad (15)$$

139 The electrophilic index is expressed as [17, 18];

140 
$$\omega = \frac{\mu^2}{2\eta} \quad (16)$$

### 141 2.3 Non-Linear Optical Properties

142 In order to gain an insight on the effects of solvent on the non-linear optical properties (NLO) of  
 143 **perylene; the dipole** moment, polarizability, anisotropic polarizability and hyperpolarizability  
 144 were calculated.

145 Dipole moment is a property used in describing the polarity of a system. For molecular systems,  
 146 this property can be obtained from[19];

147 
$$\mu_{tot} = [\mu_x^2 + \mu_y^2 + \mu_z^2]^{1/2} \quad (17)$$

148 where  $\mu_x$ ,  $\mu_y$  and  $\mu_z$  are the components of the dipole moment in x, y and z coordinates.

149 Electric dipole polarizability is an important property used in determining the polarizability of a  
 150 molecule or compound. It is a measure of the linear response of an infinitesimal electric field (F)  
 151 and represents second-order variation energy [20];

152 
$$\alpha = -\frac{\partial^2 E}{\partial F_a \partial F_b} \quad (18)$$

153 where a, and b are coordinates of x, y and z. The mean polarizability is calculated using [16];

154 
$$\alpha = \frac{1}{3}(\alpha_{xx} + \alpha_{yy} + \alpha_{zz}) \quad (19)$$

155 where the  $\alpha_{xx}$ ,  $\alpha_{yy}$  and  $\alpha_{zz}$  quantities are known as principal values of polarizability tensor.

156 The anisotropic polarizability is given **by [17]:**

157 
$$\Delta\alpha = \left[ \frac{(\alpha_{xx} - \alpha_{yy})^2 + (\alpha_{yy} - \alpha_{zz})^2 + (\alpha_{zz} - \alpha_{xx})^2 + 6(\alpha_{xz}^2 + \alpha_{xy}^2 + \alpha_{yz}^2)}{2} \right]^{1/2} \quad (20)$$

158 The mean first hyperpolarizability is **defined as [17, 21]:**

159 
$$\beta_{tot} = (\beta_x^2 + \beta_y^2 + \beta_z^2)^{1/2} \quad (21)$$

160 where  $\beta_x$ ,  $\beta_y$  and  $\beta_z$  are defined as:

161 
$$\beta_x = \beta_{xxx} + \beta_{xyy} + \beta_{xzz}$$

162 
$$\beta_y = \beta_{yyy} + \beta_{xxy} + \beta_{yzz}$$

163 
$$\beta_z = \beta_{zzz} + \beta_{xxz} + \beta_{yyz} \quad (22)$$

164 The  $\beta_x$ ,  $\beta_y$  and  $\beta_z$  refer to the components of hyperpolarizability along x, y and z components of  
165 molecular dipole moment.

#### 166 2.4 Natural Bond Orbital (NBO)

167 NBO analysis provides an efficient method for studying intra and intermolecular bonding  
168 interactions among bonds, and also provides a convenient basis for investigation of charge  
169 transfer or conjugative interactions in molecular systems [22]. The second-order Fock matrix is  
170 used to evaluate the donor-acceptor interactions in the NBO basis. For each donor and acceptor,  
171 the stabilization energy  $E^{(2)}$  associated with the electron delocalization between donor and  
172 acceptor is estimated as [23];

173 
$$E^{(2)} = -n_\sigma \frac{\langle \sigma | F | \sigma^* \rangle^2}{\varepsilon_{\sigma^*} - \varepsilon_\sigma} = -n_\sigma \frac{F_{ij}^2}{\Delta E} \quad (23)$$

174 where  $\langle \sigma | F | \sigma^* \rangle^2$ , or  $F_{ij}^2$  is the Fock matrix element between i and j NBO orbitals,  $\varepsilon_{\sigma^*}$  and  $\varepsilon_\sigma$  are  
175 the energies of  $\sigma^*$  and  $\sigma$  NBO's and  $n_\sigma$  is the population of the donor orbital.

### 176 3. COMPUTATIONAL METHOD

177 Geometry of perylene was optimized with no symmetry constraint using Becke's three-  
178 parameter hybrid exchange [24] combined with Lee-Yang-Parr's gradient-corrected correlation  
179 [25] functional (B3LYP) method with 6-311++G(d,p) basis set. All the parameters were fully  
180 allowed to relax and each of the calculations converged to an optimized geometry which  
181 corresponds to a true energy minimum.

182 For the study of solvation effects, a Self-Consistent Reaction Field (SCRF) approach based on  
183 Polarizable Continuum Model (PCM) were employed. The effects of four solvents (water,  
184 chloroform, benzene and acetone) were investigated by means of the SCRF method based on  
185 PCM as implemented in the Gaussian 03 [26]. The optimized geometries were then used to  
186 obtain the HOMO-LUMO energy gap, chemical hardness, chemical softness, chemical potential,  
187 electronegativity, electrophilicity index, dipole moment, polarizability, anisotropic polarizability,  
188 hyperpolarizability, entropy and the specific heat capacity of the investigated molecule at the  
189 same level of theory (B3LYP/6-311++G(d,p)). Finally, the NBO calculations [27] were  
190 performed using NBO 3.1 program as implemented in the Gaussian 03 package at same level of  
191 theory in order to understand the various second-order interactions between the filled orbitals of  
192 one subsystem and the vacant orbitals of another subsystem. All calculations were performed  
193 within the framework of Density Functional Theory (DFT) as coded in Gaussian 03 package  
194 [26].

## 195 4. RESULTS AND DISCUSSION

### 196 4.1 Optimized Parameters

197 The optimized values of bond lengths and bond angles of the studied molecule were calculated at  
198 DFT/B3LYP level using 6-311++G(d,p) basis set in the gas phase and in different solvents  
199 (water, chloroform, benzene and acetone). The results are shown in Tables 1 and 2. The distance  
200 between the nuclei of two atoms bonded together is termed as bond length while bond angle is  
201 the angle between two adjacent bonds of an atom in a molecule [20].

202 From Table 1, there are little changes in the bond lengths of Perylene when optimized with  
203 water, chloroform, benzene and acetone compared with the gas phase. The result shows that the  
204 lowest value obtained was 1.0825 Å in benzene. However, when compared with results of an  
205 **isolated perylene molecule [6], the bond lengths here tend to be a little smaller. It is worth** noting  
206 that, the smaller the bond length, the higher the bond energy and stronger the bond [28].  
207 Consequently, this has affirmed that the bond **lengths of perylene in** the gas phase and in solvents  
208 are a little stronger than that of an **isolated perylene molecule.** Hence, an enormous amount of  
209 energy is required to break these bonds. It was also observed that the bond length increases with  
210 an increase in the polarity of the solvents.

211 **Table 1:** Selected bond lengths (Å) of the optimized structure of perylene in the gas phase and in  
 212 different solvents.

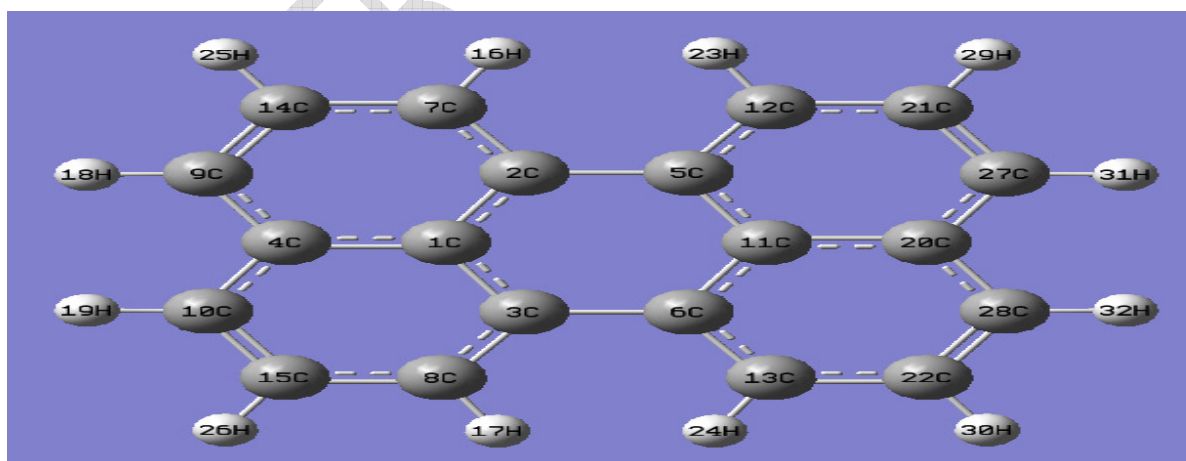
Bond Lengths (Å)	Gas Phase	Water	Chloroform	Benzene	Acetone	Previous Work
R(2,5)	1.4762	1.4773	1.4769	1.4765	1.4772	1.4700 <sup>a</sup>
R(1,4)	1.4339	1.4346	1.4342	1.434	1.4345	1.4360 <sup>a</sup>
R(1,2)	1.4315	1.4324	1.4319	1.4316	1.4323	1.4310 <sup>a</sup>
R(28,32)	1.0858	1.0877	1.0866	1.0858	1.0875	1.0900 <sup>a</sup>
R(14,25)	1.0853	1.0872	1.0862	1.0854	1.087	1.0900 <sup>a</sup>
R(13,24)	1.0827	1.0846	1.0833	1.0825	1.0841	1.0900 <sup>a</sup>

213 <sup>a</sup>[6]

214 **Table 2:** Selected bond angles (°) of the optimized structure of perylene in the gas phase and in  
 215 different solvents.

Bond Angles (°)	Gas Phase	Water	Chloroform	Benzene	Acetone
A(6,3,8)	122.184	122.106	122.130	122.143	122.119
A(3,8,15)	122.001	121.870	121.918	121.944	121.890
A(14,9,18)	120.748	120.919	120.866	120.838	120.900
A(11,20,27)	119.592	119.640	119.626	119.612	119.639
A(20,28,32)	118.965	118.859	118.894	118.905	118.876
A(14,7,16)	117.706	117.733	117.717	117.759	117.679

216



217

218 **Fig.1** Optimized Structure of Perylene

219 However, the longest bond length is 1.477Å, which is almost the same in both gas phase and  
220 solvents. The structural geometry of the studied molecule that consists of bond lengths and bond  
221 angles are found to be in good agreement with those from previous work [6]. But in [6] the  
222 molecule is in the form of an isolated perylene, diindol[1,2,3-cd:1',2',3'-Im]perylene (DIP)  
223 molecule and DIP molecular crystal.

#### 224 4.2 Frontier Molecular Orbital Energies (FMOEs)

225 Table 3 presents the highest occupied molecular orbital (HOMO), the lowest unoccupied  
226 molecular orbital (LUMO) and HOMO and LUMO energy gaps of perylene in the gas phase and  
227 in solvents calculated at the DFT/B3LYP level in the 6-311++G(d,p) basis set. The values of  
228 HOMO, LUMO and their energy gaps reflect the chemical activity of the molecule. The energy  
229 gap between HOMO and LUMO determines the kinetic stability, chemical reactivity, optical  
230 polarizability and chemical hardness-softness of a molecule [21]. Compounds with large  
231 HOMO-LUMO gap value tend to have higher stability [18]. In this work, the order of stability of  
232 the molecule is more in the gas phase > water > acetone > chloroform > benzene. Interestingly, the  
233 order of stability increases with an increase in polarity of the solvents.

234 HOMO as an electron donor represents the ability to donate an electron, while LUMO as an  
235 electron acceptor represents the ability to accept an electron. The smaller the LUMO and HOMO  
236 gaps, the easier it is for the HOMO electron to be excited; the higher the HOMO energies, the  
237 easier it is for HOMO to donate electrons; the lower the LUMO energies, the easier it is for the  
238 LUMO to accept electrons [29].

239 It can be observed from Table 3, that the LUMO energy of perylene in benzene (-2.2829 eV) is  
240 smaller than that in the gas phase and in the rest of the solvents. Hence, the electron transfer from  
241 HOMO to LUMO of the molecule in benzene is relatively easier than that in the gas phase and in  
242 the rest of the solvents. It can also be observed that the HOMO and energy gap of perylene  
243 increases with increase in polarity of the solvents.

244 The HOMO-LUMO gap of 2.976 eV obtained in the gas phase is found to be very close to 2.972  
245 eV of an isolated Perylene reported by [6].

246 **Table 3:** Calculated HOMO, LUMO and energy gap in (eV) of the optimized structure of  
 247 perylene in the gas phase and different solvents using B3LYP methods with 6-311++G(d,p) basis  
 248 set.

Solvents	$E_{HOMO}$ (eV)	$E_{LUMO}$ (eV)	Gap (eV)	Previous Work
Gas Phase	-5.2693	-2.2757	2.9935	2.9740 <sup>a</sup> 2.98 <sup>b</sup>
Water	-5.3227	-2.3332	2.9895	
Chloroform	-5.2878	-2.3005	2.9873	
Benzene	-5.2729	-2.2829	2.9860	
Acetone	-5.3167	-2.3274	2.9893	

249 <sup>a</sup>[6] <sup>b</sup>[5]

### 250 4.3 Total Ground State Energy

251 **Table 4 presents the** dielectric constants of the solvents and total energy in atomic mass unit (a.u)  
 252 of Perylene molecule in the gas phase and in different solvents calculated at the DFT/B3LYP  
 253 level with 6-311++G(d,p) basis set. The ground state total energy is an important property that  
 254 describes the physical properties of a molecule. It can be seen **from Table 4 that** the ground state  
 255 total energy increases with an increase in dielectric constant of the solvents.

256 **Table 4:** Ground state total energies in atomic mass unit (a.u) of the optimized structure of  
 257 perylene in the gas phase and different solvents.

Solvents	B3LYP/6- 311++G(d,p)	$\epsilon$
Gas Phase	-769.5611634	-
Water	-769.5983746	80.37
Chloroform	-769.5914965	4.806
Benzene	-769.5874674	2.284
Acetone	-769.5954100	37.50

258

### 259 4.4 Ionization Potentials and Electron Affinity

260 The ionization potential (IP) and electron affinity (EA) measure the tendency of compounds to  
 261 lose or gain an electron [30]. The IPs and EAs are presented in Table 5. The higher the ionization

262 potential (IP), the more difficult it is to remove an electron to form an ion. The lower the electron  
263 affinity (EA), the less easy it is to add an electron.

264 In Table 5, it can be observed that it is more difficult to remove an electron from water>  
265 acetone> chloroform> benzene> gas phase to form an ion. Similarly, it is more difficult to add an  
266 electron in terms of their EAs to the molecule in gas phase> benzene>chloroform> acetone  
267 >water. It was observed that the ionization potential increases with an increase in the polarity of  
268 the solvents while the electron affinity decreases as the polarity of the solvents decreases. Non-  
269 polar hydrocarbon molecules such as perylene are hydrophobic (water fearing) in nature. Water  
270 and some other polar solvents are unable to form significant attractive interactions with non polar  
271 molecules in which the carbon and hydrogen atoms are well bonded together through non polar  
272 vander waals interactions. In other words the energy derived from the interactions of polar  
273 solvents and non polar organic molecule is not enough to breakup the ion-ion interaction within  
274 the molecule.

275

276

277 **Table 5:** Ionization potentials and electron affinities of the optimized structure of a perylene  
278 molecule in the gas phase and different solvents.

Solvents	IP (eV)	EA (eV)
Gas Phase	5.2693	2.2757
Water	5.3227	2.3332
Chloroform	5.2878	2.3005
Benzene	5.2729	2.2829
Acetone	5.3167	2.3274

#### 279 4.5 Global Chemical Indices

280 The global chemical indices such as chemical hardness, chemical softness, chemical potential,  
281 electronegativity and electropilicity index of the molecule in the gas phase and in different  
282 solvents were computed and reported in Table 5 using the frontier molecular orbital energy.

283 **Table 6:** Global chemical indices of the optimized Perylene in the gas phase and in different  
 284 solvents.

Solvents	$\eta$ (eV)	S (eV)	$\chi$ (eV)	$\mu$ (eV)	$\omega$ (eV)
Gas Phase	1.4968	0.6680	3.7725	-3.7725	4.7540
Water	1.4948	0.6690	3.8279	-3.8279	4.9013
Chloroform	1.4937	0.6695	3.7942	-3.7942	4.8188
Benzene	1.4950	0.6689	3.7772	-3.7772	4.7734
Acetone	1.4947	0.6690	3.8221	-3.8221	4.8867

285  
 286 Chemical hardness is proportional to the HOMO-LUMO energy gap. An Increase in the  
 287 chemical hardness makes the molecule more stable and less reactive. As seen in Table 6,  
 288 Perylene molecule **in the gas phase with slightly higher value of** chemical hardness of 1.4968eV  
 289 is considered to be harder and more stable than in the rest of the solvents, followed by benzene,  
 290 water and acetone with chemical hardness of 1.4950eV, 1.4948eV and 1.4947eV respectively.  
 291 This indicates that Perylene in chloroform is more stable than in the rest of the solvents.

#### 293 4.6 Thermodynamic Properties

294 **Table 7 presents** the components and total contribution of the electronic, translational, rotational  
 295 and vibrational energies to the entropy (S) and heat capacity (Cv) as well as the rotational  
 296 constants and zero-point vibrational energies (ZPVE) of Perylene in the gas phase and in  
 297 different solvents.

298 **Table 7:** Thermodynamic properties of the optimized structure of perylene in the gas phase and  
 299 different solvents.

Positions	Gas Phase		Water		Chloroform		Benzene		Acetone	
	Cv (Kcal/Mol)	S (Kcal/Mol)	Cv (Kcal/Mol)	S (Kcal/Mol)	Cv (Kcal/Mol)	S (Kcal/Mol)	Cv (Kcal/Mol)	S (Kcal/Mol)	Cv (Kcal/Mol)	S (Kcal/Mol)
Electronic	0	0	0	0	0	0	0	0	0	0
Translational	2.981	42.474	2.981	42.474	2.981	42.474	2.981	42.474	2.981	42.474
Rotational	2.981	33.24	2.981	33.24	2.981	33.24	2.981	33.24	2.981	33.24

nal		2		6		4		3		6
Vibrational	50.951	37.398	50.961	36.331	50.939	36.745	50.913	37.045	50.964	36.454
Total	56.913	113.114	56.922	112.051	56.901	112.463	56.875	112.762	56.925	112.174
Rotational Constants (GHz)	0.62504	0.62372		0.62427		0.62464		0.62388		
	0.3306	0.33026		0.33042		0.33056		0.33027		
	0.21623	0.21593		0.21606		0.21616		0.21595		
ZPVE (Kcal/Mol)	158.55182	157.37117		157.80191		158.12372		157.48719		

300

301 It can be observed in Table 7 that specific heat capacity of perylene is found to increase with an  
 302 increase in the polarity of the solvents, while the entropy decreases as the dielectric constant  
 303 increases. The zero-point vibrational energy (ZPVE) decreases with an increase in the polarity of  
 304 the solvents.

305

#### 306 4.7 Non-Linear Optical Properties

307 Our investigation also highlighted the effects of solvents on the nonlinear optical properties of  
 308 the molecule. This is necessary for sufficient understanding of the nonlinear optical response of  
 309 the molecule. Nonlinear optical (NLO) effect arises from the interactions of electromagnetic  
 310 fields in various media to produce new fields altered in phase, frequency, amplitude and other  
 311 propagation characteristics from the incident fields [31].

312 **Table 8 presents** the non-linear optical properties in atomic mass unit (a.u) **of perylene molecule**  
 313 in the gas phase and in solvents. The properties computed and reported are dipole moment ( $\mu_{tot}$ ),  
 314 polarizability ( $\langle\alpha\rangle$ ), anisotropic polarizability ( $\Delta\alpha$ ) and hyperpolarizability ( $\beta_{tot}$ ).

315 **Table 8:** Non-linear optical properties (in Debye) of the optimized perylene molecule in the gas  
 316 phase and different solvents.

Solvents	$\mu_{tot}$	$\langle\alpha\rangle$	$\langle\Delta\alpha\rangle$	$\beta_{tot}$
----------	-------------	------------------------	------------------------------	---------------

Gas Phase	0.0000	108.2104	24.4360	1.00 E-4
Water	0.0000	104.3552	31.0839	4.36 E-4
Chloroform	0.0000	105.9012	28.2349	3.00 E-4
Benzene	0.0000	107.0436	26.1246	1.41 E-4
Acetone	0.0000	104.6985	30.4309	2.83 E-4

317  
318 The dipole moment in a molecule is an important electronic property which results from non-  
319 uniform distribution of charges on the various atoms in the molecule [21]. It can be observed in  
320 **Table 8 that perylene** is a neutral molecule with a dipole moment of **0.000eV both in the gas**  
321 **phase and in the solvents**. It can also be observed that the polarizability of Perylene increases as  
322 the polarity of the solvents decreases whereas the anisotropic polarizability increases with an  
323 increase in the polarity of the solvents. Consequently, increasing or decreasing the polarity of the  
324 solvents plays a significant role in determining the values of the non-linear optical properties of  
325 **perylene**.

#### 326 327 **4.8 Natural Bond Orbital (NBO) Analysis**

328 Natural Bond Orbital (NBO) analysis provides an efficient method for studying intra-and inter-  
329 molecular interaction among bonds and also provides a convenient basis for investigating charge  
330 transfer or conjugative interactions in molecular systems. Table 9 **presents the results of Natural**  
331 **Bond Orbital analysis of the optimized structure of perylene molecule** in the gas phase and in  
332 different solvents.

333 **Table 9:** Natural Bond Orbital (NBO) of optimized perylene molecule in the gas phase and in  
334 different solvents.

Donor NBO (i)	Acceptor NBO (j)	$E^{(2)}$ Kcal/mol	$E(j)-E(i)$ a.u	Fji a.u	Donor NBO (i)	Acceptor NBO (j)	$E^{(2)}$ Kcal/mol	$E(j)-E(i)$ a.u	Fji a.u
Water					Chloroform				
$\sigma$ C2-C5	$\sigma^*$ C1-C2	1.40	1.18	0.036	$\sigma$ C2-C5	$\sigma^*$ C1-C3	4.29	1.16	0.052
$\sigma$ C2-C5	$\sigma^*$ C1-C4	4.03	1.18	0.062	$\sigma$ C2-C5	$\sigma^*$ C1-C4	3.88	1.16	0.060
$\sigma$ C2-C5	$\sigma^*$ C2-C7	2.81	1.22	0.052	$\sigma$ C2-C5	$\sigma^*$ C2-C5	3.27	1.10	0.054
$\sigma$ C2-C5	$\sigma^*$ C5-C11	2.33	1.16	0.046	$\sigma$ C2-C5	$\sigma^*$ C2-C7	4.49	1.21	0.066
$\sigma$ C2-C5	$\sigma^*$ C5-C12	3.74	1.20	0.057	$\sigma$ C2-C5	$\sigma^*$ C3-C8	2.27	1.23	0.047
$\sigma$ C2-C5	$\sigma^*$ C7-	1.95	1.21	0.044	$\sigma$ C2-C5	$\sigma^*$ C4-	2.41	1.18	0.048

	C14					C10			
$\sigma$ C2-C5	$\sigma^*$ C11-C20	2.66	1.22	0.049	$\sigma$ C2-C5	$\sigma^*$ C5-C12	2.30	1.23	0.048
$\sigma$ C2-C5	$\sigma^*$ C12-C21	1.87	1.20	0.042	$\sigma$ C2-C5	$\sigma^*$ C7-H16	2.37	1.11	0.046
$\sigma$ C11-C20	$\sigma^*$ C2-C5	2.61	1.13	0.049	$\sigma$ C11-C20	$\sigma^*$ C2-C5	3.10	1.09	0.052
$\sigma$ C11-C20	$\sigma^*$ C3-C6	2.58	1.11	0.048	$\sigma$ C11-C20	$\sigma^*$ C3-C6	2.91	1.09	0.050
$\sigma$ C11-C20	$\sigma^*$ C5-C11	4.04	1.17	0.062	$\sigma$ C11-C20	$\sigma^*$ C5-C11	3.07	1.16	0.053
$\sigma$ C11-C20	$\sigma^*$ C6-C11	3.89	1.17	0.060	$\sigma$ C11-C20	$\sigma^*$ C6-C11	3.36	1.15	0.056
$\sigma$ C11-C20	$\sigma^*$ C20-C27	2.69	1.20	0.051	$\sigma$ C11-C20	$\sigma^*$ C20-C27	3.73	1.18	0.060
$\sigma$ C11-C20	$\sigma^*$ C20-28	2.71	1.20	0.051	$\sigma$ C11-C20	$\sigma^*$ C20-C28	3.72	1.18	0.060
$\sigma$ C11-C20	$\sigma^*$ C27-H31	2.35	1.11	0.046	$\sigma$ C11-C20	$\sigma^*$ C27-H31	1.81	1.10	0.040
$\sigma$ C11-C20	$\sigma^*$ C28-H32	2.36	1.11	0.046	$\sigma$ C11-C20	$\sigma^*$ C28-H32	1.85	1.10	0.041
Benzene					Gas Phase				
$\sigma$ C1-C2	$\sigma^*$ C1-C3	4.31	1.16	0.063	$\sigma$ C1-C2	$\sigma^*$ C1-C3	4.30	1.16	0.063
$\sigma$ C1-C2	$\sigma^*$ C1-C4	4.31	1.17	0.063	$\sigma$ C1-C2	$\sigma^*$ C1-C4	4.31	1.17	0.063
$\sigma$ C1-C2	$\sigma^*$ C2-C5	2.49	1.12	0.047	$\sigma$ C1-C2	$\sigma^*$ C2-C5	2.49	1.12	0.047
$\sigma$ C1-C2	$\sigma^*$ C2-C7	3.75	1.25	0.061	$\sigma$ C1-C2	$\sigma^*$ C2-C7	3.75	1.25	0.061
$\sigma$ C1-C2	$\sigma^*$ C3-C8	2.29	1.21	0.047	$\sigma$ C1-C2	$\sigma^*$ C3-C8	2.29	1.21	0.047
$\sigma$ C1-C2	$\sigma^*$ C4-C10	2.67	1.20	0.051	$\sigma$ C1-C2	$\sigma^*$ C4-C10	2.67	1.20	0.051
$\sigma$ C1-C2	$\sigma^*$ C5-C12	2.23	1.21	0.047	$\sigma$ C1-C2	$\sigma^*$ C5-C12	2.23	1.21	0.047
$\sigma$ C1-C2	$\sigma^*$ C7-H16	2.42	1.12	0.047	$\sigma$ C1-C2	$\sigma^*$ C7-H16	2.45	1.11	0.047
$\sigma$ C11-C20	$\sigma^*$ C2-C5	3.07	1.12	0.052	$\sigma$ C11-C20	$\sigma^*$ C2-C5	3.06	1.12	0.052
$\sigma$ C11-C20	$\sigma^*$ C3-C6	2.24	1.11	0.045	$\sigma$ C11-C20	$\sigma^*$ C3-C6	2.24	1.11	0.045
$\sigma$ C11-C20	$\sigma^*$ C5-C11	4.25	1.16	0.063	$\sigma$ C11-C20	$\sigma^*$ C5-C11	4.24	1.16	0.063
$\sigma$ C11-C20	$\sigma^*$ C6-C11	3.95	1.16	0.061	$\sigma$ C11-C20	$\sigma^*$ C6-C11	3.94	1.16	0.061
$\sigma$ C11-C20	$\sigma^*$ C20-C27	3.83	1.18	0.060	$\sigma$ C11-C20	$\sigma^*$ C20-C27	3.86	1.18	0.060
$\sigma$ C11-C20	$\sigma^*$ C20-C28	4.03	1.19	0.062	$\sigma$ C11-C20	$\sigma^*$ C20-C28	4.06	1.19	0.062
$\sigma$ C11-C20	$\sigma^*$ C27-	1.92	1.10	0.041	$\sigma$ C11-C20	$\sigma^*$ C27-	1.95	1.10	0.042

C20	H31				C20	H31			
$\sigma$ C11-C20	$\sigma^*$ C28-H32	1.80	1.10	0.040	$\sigma$ C11-C20	$\sigma^*$ C28-H32	1.83	1.10	0.040
Acetone									
$\sigma$ C1-C2	$\sigma^*$ C1-C3	4.30	1.16	0.063					
$\sigma$ C1-C2	$\sigma^*$ C1-C4	3.89	1.16	0.060					
$\sigma$ C1-C2	$\sigma^*$ C2-C5	3.27	1.10	0.054					
$\sigma$ C1-C2	$\sigma^*$ C2-C7	4.48	1.21	0.066					
$\sigma$ C1-C2	$\sigma^*$ C3-C8	2.27	1.23	0.047					
$\sigma$ C1-C2	$\sigma^*$ C4-C10	2.24	1.18	0.048					
$\sigma$ C1-C2	$\sigma^*$ C5-C12	2.31	1.23	0.048					
$\sigma$ C1-C2	$\sigma^*$ C7-H16	2.34	1.12	0.046					
$\sigma$ C11-C20	$\sigma^*$ C2-C5	3.11	1.09	0.052					
$\sigma$ C11-C20	$\sigma^*$ C3-C6	2.92	1.09	0.051					
$\sigma$ C11-C20	$\sigma^*$ C5-C11	3.07	1.16	0.053					
$\sigma$ C11-C20	$\sigma^*$ C6-C11	3.37	1.15	0.056					
$\sigma$ C11-C20	$\sigma^*$ C20-C27	3.71	1.18	0.060					
$\sigma$ C11-C20	$\sigma^*$ C20-C28	3.70	1.18	0.059					
$\sigma$ C11-C20	$\sigma^*$ C27-H31	1.78	1.10	0.040					
$\sigma$ C11-C20	$\sigma^*$ C28-H32	1.38	1.10	0.040					

335  
336 The larger  $E^{(2)}$  value, the more intensive is the interaction between electron donors and  
337 acceptors. The more donation tendency from electron donors to electron acceptors, the greater is  
338 the extent of conjugation of the whole system [23]. It can be seen from Table 9 that the largest  
339 value of stabilization (4.49 Kcal/mol) energy  $E^{(2)}$  of perylene was obtained in chloroform.  
340 Hence, there is high intensive interactions between  $\sigma$ C1-C2 and  $\sigma^*$ C2-C7 and has greater  
341 conjugation in the molecule. The order of this interaction is more in  
342 Chloroform>Acetone>Benzene>Gas Phase>Water. This phenomenon occurs as the polarity  
343 decreases between chloroform and benzene.

344

## 345 5. CONCLUSION

346 To understand the effects of solvents on structural, electronic, thermodynamic and non-linear  
347 optical properties of Perylene molecule, we have carried out an extensive computational study of  
348 the HOMO, LUMO, HOMO-LUMO energy gap, ionization potential, electron affinity, chemical  
349 hardness, chemical softness, chemical potential, electronegativity, electrophilicity index, dipole  
350 moment, polarizability, anisotropic polarizability, hyperpolarizability, entropy, heat capacity,  
351 rotational constants and zero-point vibrational energy using the B3LYP methods under 6-  
352 311++G(d,p) basis set.

353 In the structural properties calculations, Our findings revealed that the bonds of perylene tend to  
354 be stronger in the gas phase and in solvents compared to that of an isolated perylene as reported  
355 in the literature. It was observed that the bond lengths increases with an increase in the polarity  
356 of the solvents, while the bond angles were found to increase as the polarity of the solvents  
357 decreases. In the global quantities calculations, it was found that the electron transfer from  
358 HOMO to LUMO was found to be relatively easier in chloroform than in the gas phase and in the  
359 rest of the solvents. The global quantities, HOMO and HOMO-LUMO energy gaps were found  
360 to increase as the polarity of the solvents increases. The ground state energy of perylene  
361 increases with decrease in polarity of the solvents.

362 In the Thermodynamic part of our work the specific heat capacity of Perylene increases with an  
363 increase in the polarity of the solvents while the entropy and the zero-point vibrational energy  
364 decreases as the polarity of the molecule increases. In the non-linear optical properties  
365 calculations, the polarizability increases with decrease in the dielectric constant of the solvents  
366 while the anisotropic polarizability increases as the polarity of the solvents increases. In the NBO  
367 analysis, high intensive interaction between donor and acceptor electrons was observed in  
368 chloroform due to large value of stabilization energy. The results also show that careful selection  
369 of basis set and solvents can be utilized to tune the optoelectronic properties of Perylene. The  
370 same investigation should be carried out in future for neutral and charged perylene molecule.

## 371 References

372 [1] T. Rangel, A. Rinn, S. Sharifzadeh, H. Felipe, A. Pick, and S. G. Louie, "Low-lying  
373 excited states in crystalline perylene," *PNAS*, vol. 115, no. 2, pp. 284–289, 2018.

- 374 [2] M. Burian, F. Rigodanza, H. Amenitsch, L. Almásy, I. Khalakhan, Z. Syrgiannis, and M.  
375 Prato, "Structural and Optical Properties of a Perylene Bisimide in Aqueous Media,"  
376 *Chem. Phys. Lett.*, 2017.
- 377 [3] P. Taylor and J. D. Myers, "Organic Semiconductors and their Applications in  
378 Photovoltaic Devices Organic Semiconductors and their Applications in Photovoltaic  
379 Devices," *Polym. Rev.*, pp. 37–41, 2012.
- 380 [4] J. Calbo, A. Doncel, G. Juan, and A. Enrique, "Tuning the optical and electronic  
381 properties of perylene diimides through transversal core extension," *Theor. Chem. Acc.*,  
382 vol. 137, no. 27, pp. 1–11, 2018.
- 383 [5] G. Mallocci, G. Cappellini, G. Mulas, and A. Mattoni, "Electronic and optical properties of  
384 families of polycyclic aromatic hydrocarbons : A systematic ( time-dependent ) density  
385 functional theory study," *Chem. Phys.*, vol. 384, no. 1–3, pp. 19–27, 2011.
- 386 [6] M. Mohamad, R. Ahmed, A. Shaari, and S. G. Said, "Structure - dependent optoelectronic  
387 properties of perylene , di - indenoperylene ( DIP ) isolated molecule and DIP molecular  
388 crystal," *Chem. Cent. J.*, pp. 1–9, 2017.
- 389 [7] A. Furube, M. Murai, Y. Tamaki, S. Watanabe, and R. Katoh, "Effect of Aggregation on  
390 the Excited-State Electronic Structure of Perylene Studied by Transient Absorption  
391 Spectroscopy," pp. 6465–6471, 2006.
- 392 [8] I. A. Fedorov, "Structure and electronic properties of perylene and coronene under  
393 pressure : First-principles calculations," *Comput. Mater. Sci.*, vol. 139, pp. 252–259, 2017.
- 394 [9] I. A. Fedorov, Y. N. Zhuravlev, V. P. Berveno, I. A. Fedorov, Y. N. Zhuravlev, and V. P.  
395 Berveno, "Structural and electronic properties of perylene from first principles  
396 calculations Structural and electronic properties of perylene from first," *J. Chem. Phys.*,  
397 vol. 94509, no. 138, pp. 1–6, 2013.
- 398 [10] A P. Maharolkar, A.G. Murugkar, P.W. Khirade, S.C. Mehrotra, "Study of thermophysical  
399 properties of associated liquids at 308.15 K and 313.15 K", *Russian Journal of Physical  
400 chemistry A* , 91 (9), 1710-1716, 2017.

- 401 [11] D. Sholl, *Density Functional Theory: A Practical Introduction*. Hoboken, New Jersey:  
402 John Wiley & Sons, Inc, Pp. 1, 2009.
- 403 [12] P. Giannozzi, "Lecture Notes Per Il Corso Di Struttura Della Materia ( Dottorato Di Fisica  
404 , Universit ` A Di Pisa , V . 2005 ): Density Functional Theory For Electronic Structure  
405 Calculations," Pp. 1–35, 2005.
- 406 [13] P. H. and W. Khon, "Inhomogeneous Electron Gas," *Phys. Rev.*, vol. 136, no. 3B, pp.  
407 864–870, 1964.
- 408 [14] R. M. Martin, *Electronic Structure, Basic Theory And Practical Methods*. Cambridge:  
409 Cambridge University Press, Pp. 119, 2004.
- 410 [15] R. O. Jones, "Introduction to Density Functional Theory and Exchange-Correlation  
411 Energy Functionals," *Comput. Nanosci.*, vol. 31, pp. 45–70, 2006.
- 412 [16] O. E. Oyeneyin, "Structural and Solvent Dependence of the Electronic Properties and  
413 Corrosion Inhibitive Potentials of 1 , 3 , 4-thiadiazole and Its Substituted Derivatives- A  
414 Theoretical Investigation," *Phys. Sci. Int. J.*, vol. 16, no. 2, pp. 1–8, 2017.
- 415 [17] M. F. Khan, R. Bin Rashid, A. Hossain, and M. A. Rashid, "Computational Study of  
416 Solvation Free Energy, Dipole Moment, Polarizability, Hyperpolarizability and Molecular  
417 Properties of Betulin , a Constituent of *Corypha taliera* ( Roxb .)," *Dhaka Univ. J. Pharm.*  
418 *Sci.*, vol. 16, no. 1, pp. 1–8, 2017.
- 419 [18] K. K. Srivastava, S. Srivastava, and T. Alam, "Theoretical study of the effects of solvents  
420 on the ground state of TCNQ," *Pelagia Res. Libr.*, vol. 5, no. 1, pp. 288–295, 2014.
- 421 [19] M. Targema, M. D. Adeoye, and S. T. Gbangban, "Calculation of Electronic Properties of  
422 Some 4-Nitroaniline Derivatives : Molecular Structure and Solvent Effects," *Int. Res. J.*  
423 *Pure Appl. Chem.*, vol. 8, no. 3, pp. 165–174, 2015.
- 424 [20] H. Abdulaziz, A. S. Gidado, A. Musa, and A. Lawal, "Electronic Structure and Non-  
425 Linear Optical Properties of Neutral and Ionic Pyrene and Its Derivatives Based on  
426 Density Functional Theory," *J. Mater. Sci. Rev.*, vol. 2, no. 3, pp. 1–13, 2019.

- 427 [21] D. Pegu, "Solvent Effects on Nonlinear Optical Properties of Novel Para-nitroaniline  
428 Derivatives : A Density Functional Approach," *Int. J. Sci. Res.*, vol. 3, no. 7, pp. 469–474,  
429 2014.
- 430 [22] R. P. Gangadharan, "First Order Hyperpolarizabilities , NPA and Fukui Functions . . .,"  
431 *ACTA Phys. POLANICA A*, vol. 127, no. 3, pp. 748–752, 2015.
- 432 [23] Z. Rui-zhou, L. Xiao-hong, and Z. Xian-zhou, "Molecular structure , vibrational spectra  
433 and NBO analysis on using DFT method," *Indian J. Pure Appl. Phys.*, vol. 49, no. 11, pp.  
434 731–739, 2011.
- 435 [24] A. D. Becke and A. D. Becke, "Densityfunctional thermochemistry . III . The role of exact  
436 exchange Density-functional thermochemistry . III . The role of exact exchange," *J.*  
437 *Chem. Phys.*, vol. 98, no. 7, pp. 5648–5652, 1993.
- 438 [25] R. G. P. Chengteh Lee, Weitao Yang, "Developmenet of the ColleSalvetti Correlation-  
439 Energy Formula into a Functional of the Electron Density," *Phys. Rev. B*, vol. 37, no. 2,  
440 pp. 785–789, 1988.
- 441 [26] H. M. Frisch M. J., Trucks G. W., Schlegel H. B., Scuseria G. E., Robb M. A., Cheeseman  
442 J. R., Scalmani G., Barone V., Mennucci B., Petersson G. A., Nakatsuji H., Caricato M.,  
443 X. Li, H. Hratchian P., Izmaylov A. F., Bloino J., Zheng G., Sonnenberg J. L., "Gaussian  
444 Software." Gaussian, INC, 2004.
- 445 [27] F. Glendening, E., D., Reed, A., B., Carpenter, J., E. and Wienhold, "NBO 3.1."  
446 University of Wisconsin, Madison, 1998.
- 447 [28] S. Suzuki, Y. Morita, K. Fukui, K. Sato, D. Shiomi, T. Takui, and K. Nakasuji,  
448 "Aromaticity on the Pancake-Bonded Dimer of Neutral Phenalenyl Radical as Studied by  
449 MS and NMR Spectroscopies and NICS Analysis," *J. Am. Chem. Soc.*, vol. 128, no. 8, pp.  
450 2530–2531, 2006.
- 451 [29] A. H. Mekky, H. G. Elhaes, M. M. El-okr, A. S. Al-aboodi, and M. A. Ibrahim, "Applied  
452 & Computational Mathematics Effect of Solvents on the Electronic Properties of  
453 Fullerene Based Systems : Molecular Modelling," *Applies Comput. Math.*, vol. 4, no. 1,

454 pp. 1–4, 2015.

455 [30] A. Kumer, B. Ahmed, A. Sharif, and A. Al-mamun, “A Theoretical Study of Aniline and  
456 Nitrobenzene by Computational Overview,” *Asian J. Phys. Chem. Sci.*, vol. 4, no. 2, pp.  
457 1–12, 2017.

458 [31] C. Janaki, E. Sailatha, S. Gunasekaran, and G. R. R. Kumar, “Molecular structure and  
459 spectroscopic characterization of Metformin with experimental techniques and DFT  
460 quantum chemical calculations,” *Int. J. Techno. Chem. Res.*, vol. 2, no. 2, pp. 91–104,  
461 2016.

462

463

UNDER PEER REVIEW